Marcus S. Allegood was born in Des Moines, IA and grew up in both Pensacola, FL and Dublin, GA. He attended North Georgia College and State University, majoring in Physics. During his undergraduate career he held two SULI internships and a CCI internship at the Oak Ridge National Laboratory during the summers of 2005 to 2007. He was recently accepted into the masters program at the Georgia Institute of Technology in the Medical Physics program and hopes to pursue a career as a Medical Physicist. His interests included collecting books, football, and kayaking.

Justin S. Baba is a staff research scientist and development biomedical engineer in the Engineering Science & Technology Division at Oak Ridge National Laboratory (ORNL), Tennessee. He received his Ph.D. in Biomedical Engineering, 2003 from Texas A&M University, College Station, TX and joined ORNL in Sept. 2003. His primary research focus is in non-invasive diagnostics using both ionizing and non-ionizing radiation sources. He has additional interests in the development of non-invasive optical and electronics based sensors for medical and non-medical applications.

Extension of the Inverse Adding-Doubling Method to the Measurement of Wavelength-Dependent Absorption and Scattering Coefficients of Biological Samples

Marcus S. Allegood and Justin S. Baba

ABSTRACT

Light interaction with biological tissue can be described using three parameters: the scattering and absorption coefficients (μ_s and μ_a), as well as the anisotropy (g) which describes the directional dependence of the scattered photons. Accurately determining these optical properties for different tissue types at specific wavelengths simultaneously would be beneficial for a variety of different biomedical applications. The goal of this project was to take a user defined g-value and determine the remaining two parameters for a specified wavelength range. A fully automated computer program and process was developed to collect data for all wavelengths in a timely and accurate manner. LabVIEW® was used to write programs to automate raw intensity data collection from a spectrometer equipped integrating sphere, conversion of the data into a format for analysis via Scott Prahl's Inverse Adding-Doubling (IAD) C code execution, and finally computation of the optical properties based on the output from the IAD code. To allow data to be passed efficiently between LabVIEW® and C code program modules, the two were combined into a single program (OPT 3.1). OPT 3.1 was tested using tissue mimicking phantoms. Determination of the absorption and scattering coefficients showed excellent agreement with theory for wavelengths where the user inputted single g-value was sufficiently precise. Future improvements entail providing for multi-wavelength g-value entry to extend the accuracy of results to encompass the complete multispectral range. Ultimately, the data collection process and algorithms developed through this effort will be used to examine actual biological tissues for the purpose of building and refining models for light-tissue interactions.

Introduction

In recent years, the need for accurate models for light-tissue interaction has led to the development of several methods for characterizing the optical properties of biological tissue samples. Of these, one that is widely utilized is an integrating sphere in conjunction with the Inverse Adding-Doubling program (IAD) developed by Scott Prahl [1]. The integrating sphere method is a process by which raw light intensity data for a particular sample can be collected. By positioning the sample at either the front or the rear port of the sphere, transmitted or reflected intensity from an incident light source can be recorded within the sphere using an appropriately mounted photo-detector. The IAD program can then take this data and apply a brute force iterative process to determine the desired values. Essentially, the numerical process entails accepting raw intensity data as inputs and then repeatedly guessing the scattering and absorption coefficients until an appropriate match is attained [1].

To date, the vast majority of methods that have been investigated, including the method developed by Prahl, are designed to collect the respective optical properties at a single wavelength via a monochromatic laser light source. The process that we have developed addresses this limitation by using a collimated white light source to allow for user specified spectral data collection. System generated multi-wavelength data is analyzed by a program that computes the respective optical properties for each wavelength within the spectrum. Because scatter and absorption theories are well established for visible wavelengths, our system is only limited by its wavelength response and resolution for the individual wavelengths emitted by the light source.

Wavelength dependent light propagation through biological tissue can be described with three parameters: the anisotropy (g)

the scattering coeffecient μ_s and absorption coefficient μ_a. The anisotropy describes the fraction of light forward scattered from an initial propagating direction *s* to *s'*. The reciprocal of the scattering (or absorption) coefficient is the average distance that a photon will travel before being scattered (or absorbed) [1]. It is these parameters that the IAD program does a particularly good job of determining. For this reason, the IAD program implemented for a single integrating sphere serves as the building block of our system. In this paper we present and discuss our developed system and the accuracy of results using tissue mimicking phantoms to test it, the underlying theory used, and the issues that arose over the course of data collection and optical property determination.

Theory

Four raw light intensity measurements are needed for each sample. The collection of the required light intensity measurements along with the corresponding variable names are illustrated in Figures 1 and 2. Figure 1 depicts collection of sample transmitted light, variable: *samp_t* (Figure 1A) and sample reflected light, variable: *samp_r* (Figure 1B). Figure 2 depicts collection of two system characterization readings that are used to remove system optical response from measured sample readings. These are variable: *tot* (Figure 2A) — accounts for total internal reflection within the sphere, and variable: *dark* (Figure 2B) — accounts for non-perfect collimation of the input light source, i.e., slight divergence of light source output rays from parallel. Figure 3 depicts collection of the system baseline parameter, variable: *base* — accounts for system electronic noise, primarily from the charge coupled device (CCD) array in the detection spectrometer.

Once raw intensity data is collected for each required variable, two new variables are created, T and R, which represent the baseline corrected and normalized light transmission and reflection intensities respectively (Equations 1 and 2). Essentially, any light not recorded as either transmitted or reflected intensity, as captured by T and R, is assumed by the program to be absorbed by the sample [1].

$$T = \frac{[(sam\_t - base) - (dark - base)]}{[(tot - base) - (dark - base)]} \quad (1)$$

$$R = \frac{[(sam\_r - base) - (dark - base)]}{[(tot - base) - (dark - base)]} \quad (2)$$

The conservation of energy condition that the sum of R and T must be equal to or less than one, in Equation 3, is implemented in the program. Therefore, all values outside this range are returned as errors by the program.

$$R + T \leq 1 \quad (3)$$

Anisotropy (g), is a value that must be predetermined and provided by the user [1]. The g-value implemented in this system, g_{HG}, is determined by the Henyey-Greenstein phase function $p(\theta)$, which describes the amount of light scattered at a particular angle. As shown in Equation 4, it varies by a factor, β, from the anisotropy, g, as determined by Mie theory for a single scattering event [3]. β is known as the isotropic factor and it accounts for the randomization of scatter that occurs due to multiple scattering events that occur in thicker samples. For simplicity, from this point forward the Henyey-Greenstein anisotropy, g_{HG}, is referred to as anisotropy unless otherwise specified.

$$g = g_{HG}(1 - \beta) \quad (4)$$

The phase function is often expressed in terms of the cosine of the scattering angle $p(\cos\theta)$ [1].

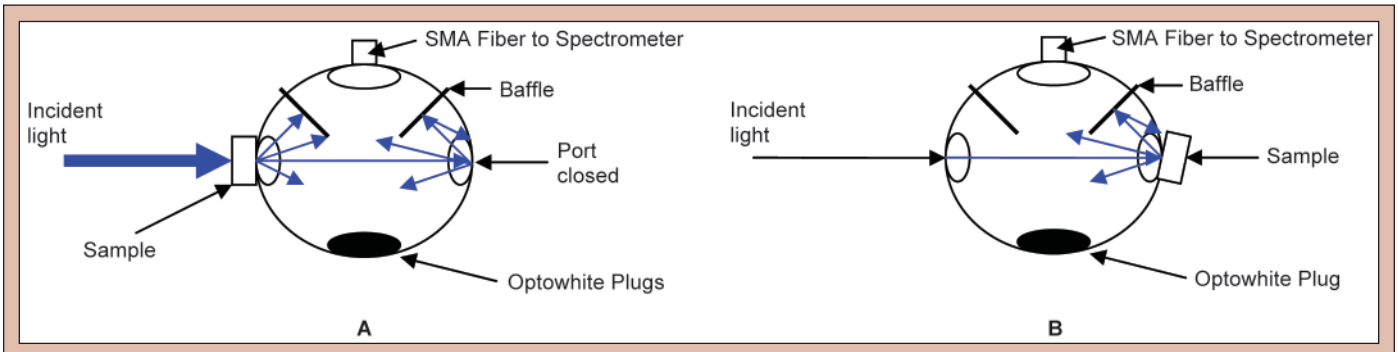

Figure 1. A. Light transmission reading. Rear port is closed (variable: *samp_t*). B. Sample reflectance reading (variable: *samp_r*).

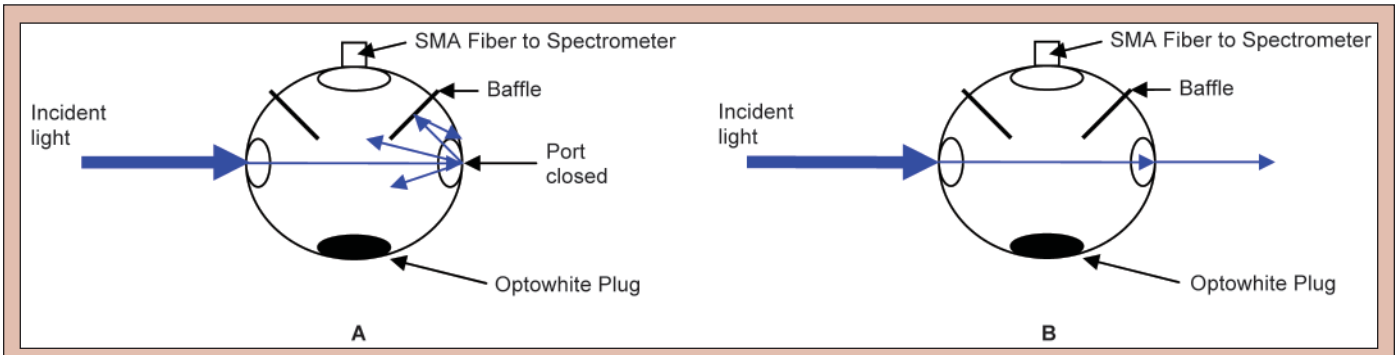

Figure 2. A. Total internal reflection. Rear port is closed (variable: *tot*). B. Optical dark reading. Both rear and front ports are open, allowing collimated beam to pass through unscattered and unabsorbed (variable: *dark*).

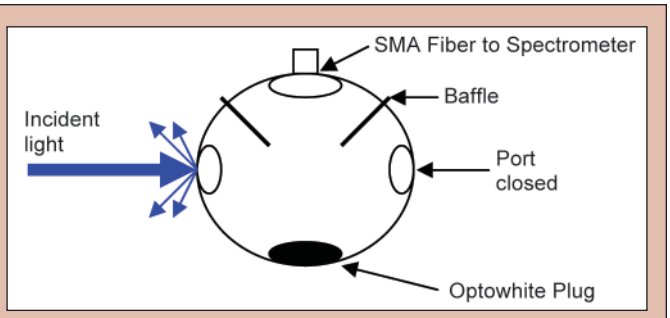

Figure 3. Baseline reading. All sphere ports are closed. This allows for system electronic noise to be subtracted out of each of the other variables (variable: *base*).

$$p(\cos\theta) = \frac{1 - g_{HG}^{\ 2}}{4\pi(1 + g_{HG}^{\ 2} - 2g_{HG}\cos\theta)^{3/2}} \tag{5}$$

The function is normalized, so that the total light intensity scattered over all angles is equal to unity.

$$\int_{4\pi} p(\cos\theta)d\omega = 1 \tag{6}$$

Calculating the expectation value of $p(\cos\theta)$ yields the anisotropy, which ranges from total isotropic scattering, i.e., $g_{HG} = 0$, and complete forward scattering, i.e., $g_{HG} = 1$.

$$\int_{4\pi} p(\cos\theta)\cos\theta d\omega = g_{HG} \tag{7}$$

The photon path is also influenced by the refractive index of both the sample holder and the sample itself. Two separate formulas are incorporated in the program for this purpose. The Cauchy equation, Equation (8), is used to determine the multispectral refractive index for the glass sample holder, while the Sellmeier equation, Equation (9), is used for actual tissue samples.

$$n(\lambda) = A + \frac{B}{\lambda^2} + \frac{C}{\lambda^4} + \ldots \tag{8}$$

$$n^2(\lambda) = 1 + \frac{A\lambda^2}{\lambda^2 - B^2} + \ldots \tag{9}$$

In both cases only the first two terms are needed as the affect due to additional terms is negligible within the visible wavelengths of interest. The Cauchy equation works extremely well for non-absorbing materials. However, it breaks down for wavelengths in the vicinity of an absorption band [6]. The Sellmeier equation begins to address this issue and was developed to account for absorption, with the second coefficient, *B*, being a wavelength equal to that of the medium's natural — i.e., primary absorptive — frequency [6]. As with anisotropy, the user must provide the coefficients for both equations. Each equation is incorporated into OPT 3.1 in order to provide the IAD program with a proper refractive index for each wavelength within the user defined range.

Normalized reflection and transmission values, *R* and *T*, and the anisotropy value, g_{HG}, provide the three main input variables for the IAD program. Given these inputs and the refractive indexes, the program applies an iterative process to arrive at a set of optical variables that match the corresponding values of *R*, *T*, and *g* that it received as inputs [1].

The optical variables output from the IAD program are the albedo (*a*) and the optical thickness (τ). Albedo, presented in Equation 10, is the ratio of the scattering coefficient to the sum of the scattering and absorption coefficients μ_s and μ_a. Highly scattering samples are dominated by μ_s and approach a limit of one, while highly absorbing samples are dominated by μ_a, and thus approach a limit of zero.

$$a = \frac{\mu_s}{(\mu_s + \mu_a)} \tag{10}$$

The optical thickness, presented in Equation 11, is the product of the sample thickness, *d*, and the sum of the scattering and absorption coefficients. It is a measure of how far a photon travels into a sample before it is either scattered or absorbed.

$$\tau = d(\mu_s + \mu_a) \tag{11}$$

With the albedo and optical thickness outputs from the IAD program as inputs, OPT 3.1 calculates μ_a and μ_s using the relationships in Equations 12 and 13.

$$\mu_a = \frac{\tau(1-a)}{d} \tag{12}$$

$$\mu_s = \frac{a\tau}{d} \tag{13}$$

The units of both the scattering and absorption coefficients are in inverse millimeters and the reciprocal of these values represents the respective mean free paths, i.e. the distance a photon travels before being either scattered or absorbed.

The results for absorption and scattering coefficients can be verified against predictions by the Beer-Lambert (Beer's) law and Mie theory respectively. The exponential form of Beer's law is presented in Equation (14) with I_0 and I_1 as the input and output intensities respectively.

$$\frac{I_0}{I_1} = e^{-A} \qquad A = \ln\left(\frac{I_1}{I_0}\right) \tag{14}$$

Absorbance, A, is related to the absorption coefficient as presented in Equation 15.

$$A = \varepsilon \cdot c \cdot l \qquad \mu_a = \varepsilon \cdot c \tag{15}$$

Here ε is the molar absorptivity [$M^{-1}mm^{-1}$] at a specific wavelength, *c* is the molar concentration [M], and *l* is the sample path length [mm]. The absorption coefficient is the product of the molar absorptivity and the concentration [4]. Mie theory is used to predict the expected values for the scattering coefficient and a well documented and free online applet is provided by Scott Prahl [5].

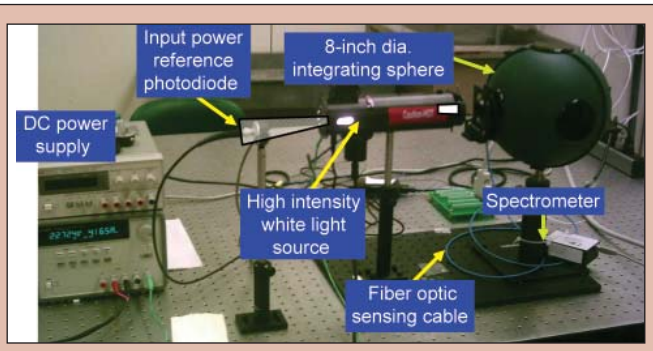

Figure 4. System hardware setup.

Materials and Methods

Experimental Setup

Figure (4) depicts the complete hardware system. It consists of a hollow 8-inch diameter sphere (SphereOptics Inc.) with a side mounted SMA fiberoptic cable that connects to an external spectrometer that utilizes a CCD detector (Ocean Optics, USB 2000). The interior walls of the sphere are coated with Optowhite ($BaSO_4$) [2] to ensure minimal absorbance and uniform photon diffusivity. By positioning a sample at the front or rear of the sphere, scattered or reflected light intensity can be recorded from an incident light source respectively. The system employs a collimated, high intensity, white light source providing a wide spectrum of wavelengths within and beyond the visible region (SphereOptics Inc., CL-100). A photodiode is also implemented externally to monitor light source power fluctuations. It provides a means to reduce intensity measurement errors via normalization of detected intensity by the corresponding light source output intensity.

LabVIEW® was used to create our OPT 3.1 program, which automated data collection over a user specified wavelength range — including a step size to extract specific wavelengths within the range. OPT 3.1 automatically calls up the IAD C code when needed, and transfers the necessary input variable data to it. Upon completion of IAD code execution, OPT 3.1 resumes control and performs the final calculations to produce the desired optical properties for each individual wavelength. The entire process is completed in a matter of minutes.

Tissue Phantoms

Tissue mimicking phantoms were produced using Trypan Blue (Sigma, T8154) to provide for absorption along with polystyrene spheres (Duke Scientific, 5100A and 5153A) to act as a scattering agent. These phantom materials were selected due to the readily available literature on their optical properties. Polystyrene sphere sizes of 1.0 and 1.5 micron diameters were utilized to mimic the strong forward scattering of biological tissues, which range in anisotropy values from 0.8 to 0.95 and are well characterized by Mie theory [1]. Sphere concentrations were chosen to be 2.97×10^9 and 1.08×10^9 parts per million (ppm) for the 1.0 and 1.5 micron spheres respectively. This was sufficient to produce accurate results and prevent skewed values seen in higher concentrations due to the level of multiple scattering events.

Samples were prepared in distilled water using different combinations of sphere sizes with varying Trypan Blue concentrations. Three sets of phantom mixtures were created. The first two sets contained only Trypan Blue or polystyrene spheres. These were used to test the system's ability to characterize samples that were either purely absorbing or scattering. They also served as reference data for comparison with samples that included both Trypan Blue and polystyrene spheres. In samples that included Trypan Blue, ten different molar concentrations were prepared ranging from 4.16×10^{-5} to 6.25×10^{-4} M. Testing was repeated three times for Trypan Blue only samples, nine times for polystyrene sphere only samples, and nine times for combination samples. All data were collected using a 1.0 mm path length sample holder constructed out of borosilicate glass.

Results and Discussion

All data presented in the following figures to be discussed were based on nine repetitions. For each, the standard deviation (σ) bars are not depicted because there are over 1,140 wavelengths sampled between 400 and 800 nm, moreover the maximum σ for all of the plotted data was determined to be ~ 4% of the nominal mean value. All spectral data were filtered to remove hot pixel values from the CCD detector output, i.e. consistently excessive spikes, and a 5 point moving average was applied for smoothing.

Absorption Coefficient, μ_a

Table 1 shows a comparison of system determined μ_a to that determined theoretically by implementing the known molar absorptivity of 6,900 $M^{-1}mm^{-1}$ at 606 nm into Equation 15 ($\mu_a|_{606}$) for ten concentrations of Trypan Blue in distilled water ranging from 4.16×10^{-5} to 6.25×10^{-4} M that were tested [7]. The results show excellent agreement to theory throughout the range of concentrations with a mean error of 2.3%. To validate system derived μ_a across the complete system spectral range, the absorbance of each solution was measured independently and modeled using Beer's law by applying

Molar Concentration [M]	Absorption coefficient, μ_a		% Error
	Theoretical	Experimental	
4.16×10^{-5}	0.287	0.277	3.5
8.33×10^{-5}	0.574	0.540	5.9
1.25×10^{-4}	0.862	0.868	0.7
1.67×10^{-4}	1.149	1.148	0.1
2.08×10^{-4}	1.437	1.413	1.7
2.50×10^{-4}	1.724	1.667	3.3
2.91×10^{-4}	2.011	1.921	4.5
3.33×10^{-4}	2.298	2.243	2.4
4.16×10^{-4}	2.872	2.808	2.2
6.25×10^{-4}	4.309	4.284	0.6
Mean			**2.3**

Table 1. Absorption coefficient comparison as a function of concentration for samples of Trypan Blue in distilled water. Theoretical values were determined from known molar absorptivity of 6,900 M^{-1} mm^{-1} at 606 nm.[13]

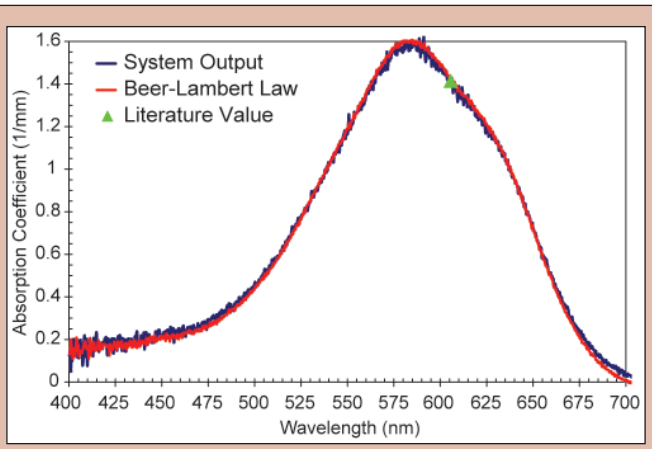

Figure 5. Absorption coefficient of Trypan Blue solution vs. wavelength comparison with a molar concentration of 2.08×10^{-4} M. The green triangle shows the value determined from the known molar absorptivity of 6,900 M^{-1} mm^{-1} at 606 nm for Trypan Blue.

Equations 14 and 15 [4]. Figure 5 shows results from a 2.08 x 10^{-4} M solution for the system spectral range of 400–700 nm. Beer's law results are represented in red, the system derived values in blue, and the green triangle shows $\mu_a|_{606}$. Again, the data shows good agreement with theory with a mean error of 2%. It should also be noted in Figure 5 that both methods converge at the $\mu_a|_{606}$ value, thus further strengthening the validity of these results. Though not presented, we consistently saw this repeated for all microsphere-Trypan Blue combinations studies. However, there are erratic values at both ends of the spectrum resulting in increased errors. These are due to hardware limitations that result in lower signal-to-noise ratios .

Data for samples that contained both an absorbing agent and a scattering agent (polystyrene microspheres) are presented in Figures 6–9. Two different samples were created using a 2.08 x 10^{-5} M concentration of Trypan Blue dye: one with 1.0 µm mean diameter spheres and the other with 1.5 µm diameter spheres. Figures 6 and 7 are the raw absorbance data for each of the samples. The red square in each figure depicts the expected value determined from the known molar absorptivity of Trypan Blue dye at 606 nm [7]. The system determined absorption coefficient values of 0.0930 and 0.0877 mm^{-1} for 1.0 and 1.5 µm diameter spheres at 606 nm. These values are in good agreement with the expected values, varying by only 4% and 0.5% respectively. Figures 8 and 9 are qualitative comparisons of normalized system absorbance values versus those determined using Beer's law.

Scattering Coefficient, μ_s

The two samples containing only polystyrene spheres, along with the two that contained both polystyrene spheres and Trypan Blue, as introduced in the absorption coefficient discussion, were utilized for investigating μ_s. The samples containing 1.0 µm spheres had a concentration of 2.97 x 10^{9} parts per mL and those with 1.5

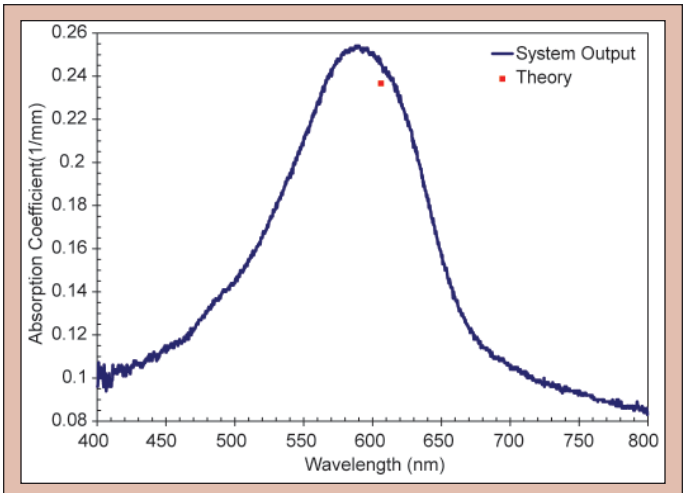

Figure 6. Absorption coefficient spectrum of Trypan Blue solution with a molar concentration of 2.08 x 10^{-4} M combined with 1.0 µm diameter polystyrene spheres. The red square shows the value determined from the known molar absorptivity of 6,900 M^{-1} mm^{-1} at 606 nm for Trypan Blue.

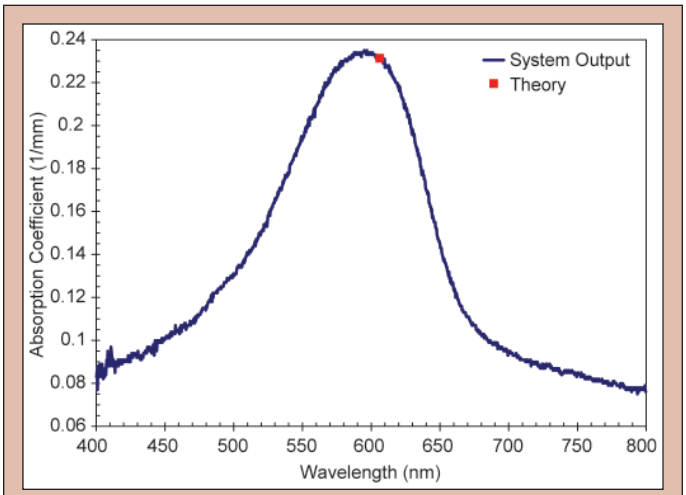

Figure 7. Absorption coefficient spectrum of Trypan Blue solution with a molar concentration of 2.08 x 10^{-4} M combined with 1.5 µm diameter polystyrene spheres. The red square shows the value determined from the known molar absorptivity of 6,900 M^{-1} mm^{-1} at 606 nm for Trypan Blue.

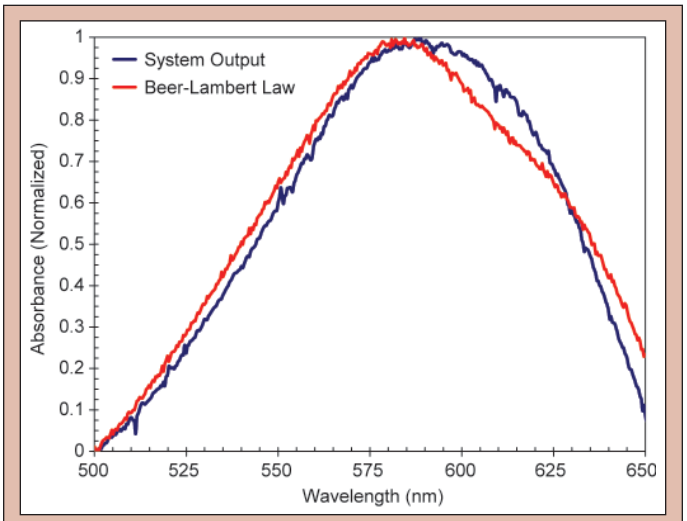

Figure 8. Normalized absorbance vs. wavelength. A comparison of system output and Beer-Lambert law modeled data for a sample consisting of a molar concentration of 2.08 x 10^{-5} M Trypan Blue combined with 1.0 µm diameter polystyrene scattering spheres.

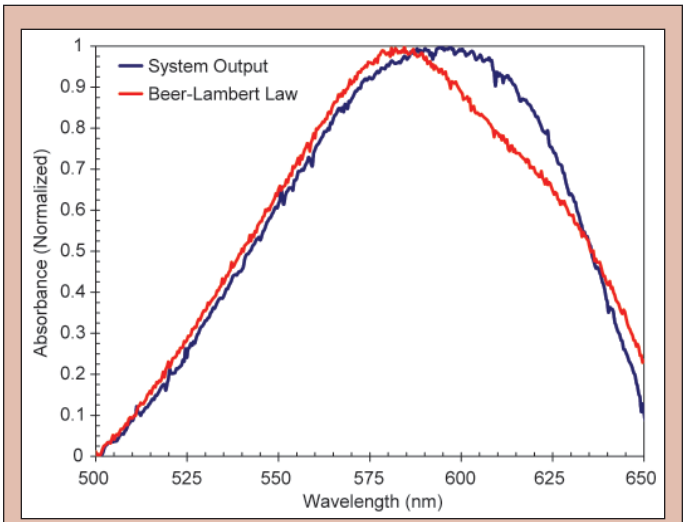

Figure 9. Normalized absorbance vs. wavelength. A comparison of system output and Beer-Lambert law modeled data for a sample consisting of a molar concentration of 2.08 x 10^{-5} M Trypan Blue combined with 1.5 µm diameter polystyrene scattering spheres.

μm sphere solutions contained 1.08 x 10^9 parts per mL. Figures 10 and 11 show data collected for the polystyrene spheres only samples. The red squares in these figures depict the expected values as determined by Mie theory [5]. The notable deviations from Mie theory are due to the current system limitation of only allowing a single anisotropy value to be specified for all wavelengths within the spectrum. However, it is well established that anisotropy varies with wavelength and this issue will be addressed in future work. The anisotropy value that was chosen for each sample was the value at 600 nm because it fell in the middle of the spectral ranges that were being examined. As such, in these figure, the best fit of the system outputted values to Mie theory occurs here.

A large deviation can be seen in the data for the 1.5 μm sphere samples. This is due to photons at the lower wavelengths approaching the geometric limit of the scattering cross section [8]. Figures 12 and 13 are the data for scattering samples that also contain a 2.08 x 10^{-5} M concentration of Trypan Blue. Again, the same deviations from theory can be seen for lower wavelengths, but there is good agreement for wavelengths that fall within the Mie regime and below the geometric limit [8].

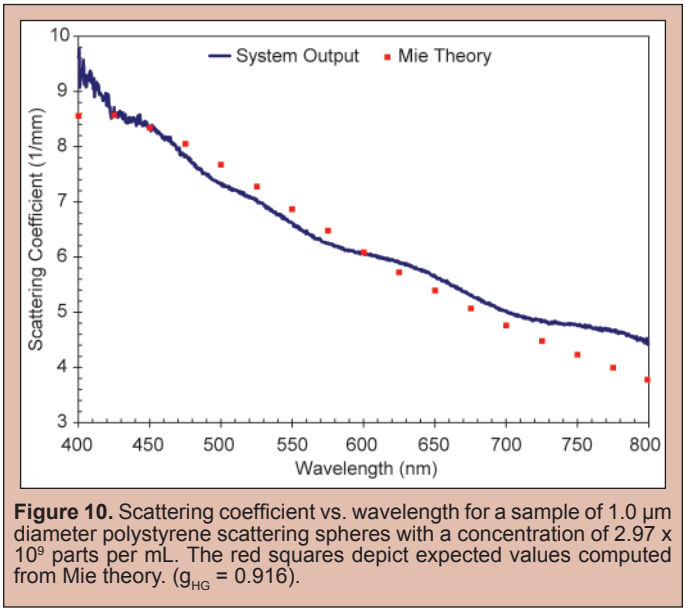

Figure 10. Scattering coefficient vs. wavelength for a sample of 1.0 μm diameter polystyrene scattering spheres with a concentration of 2.97 x 10^9 parts per mL. The red squares depict expected values computed from Mie theory. (g_{HG} = 0.916).

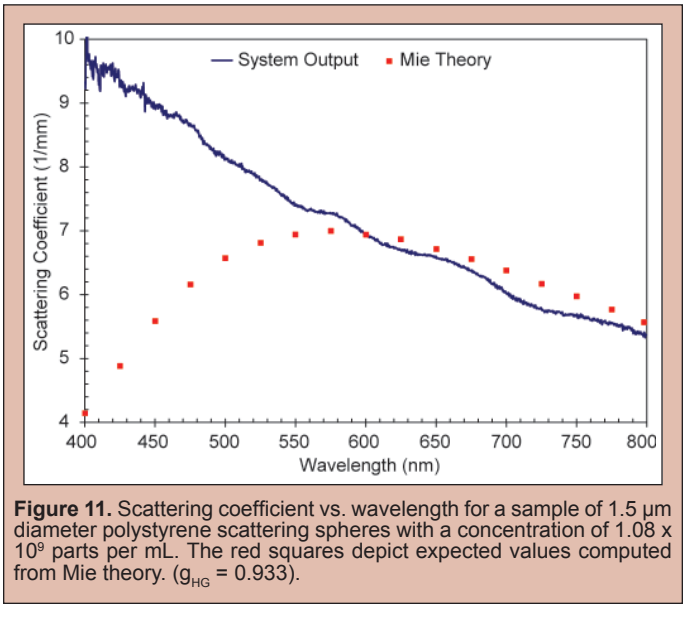

Figure 11. Scattering coefficient vs. wavelength for a sample of 1.5 μm diameter polystyrene scattering spheres with a concentration of 1.08 x 10^9 parts per mL. The red squares depict expected values computed from Mie theory. (g_{HG} = 0.933).

Conclusion and Future Work

Overall, the program performed exceptionally well for each sample tested. The system was able to reliably determine the scattering and absorption coefficients for a wide range of sample mixture concentrations. Currently, the lack of a wavelength dependent anisotropy variable in our OPT 3.1 software program is the limiting factor for accurate simultaneous characterization of a sample's multispectral optical properties. Because anisotropy varies with wavelength, as do the other parameters, accurate results are currently restricted to the wavelength range where the user-defined single *g*-value is valid. Implementing anisotropy as a wavelength dependent variable into the analysis portion of the OPT 3.1 program is the next issue to be addressed.

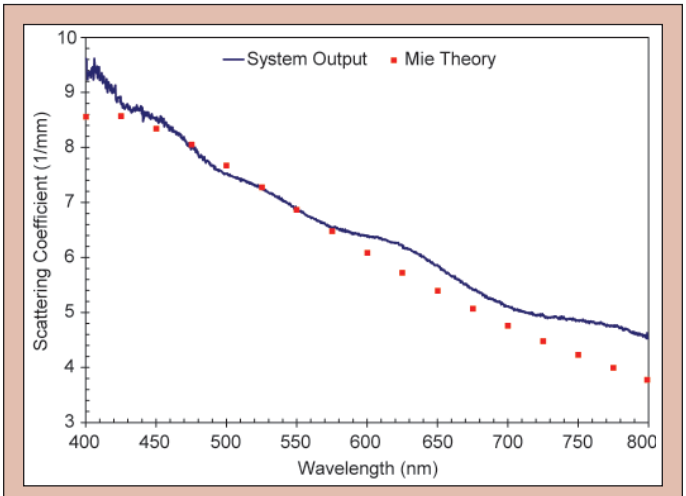

Figure 12. Scattering coefficient vs. wavelength for a sample mixture consisting of 1.0 μm diameter polystyrene scattering spheres with a concentration of 2.97 x 10^9 parts per mL and a 2.08 x 10^{-5} M concentration of Trypan Blue. The red squares depict expected values computed from Mie theory. (g_{HG} = 0.916).

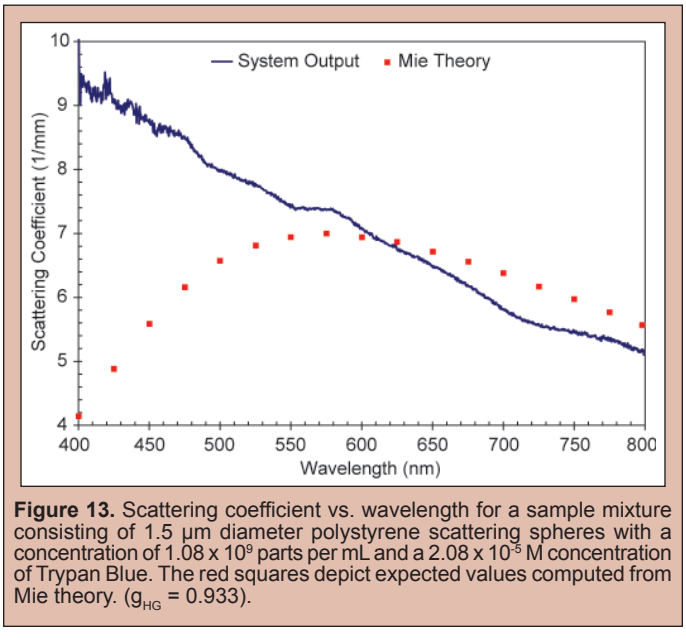

Figure 13. Scattering coefficient vs. wavelength for a sample mixture consisting of 1.5 μm diameter polystyrene scattering spheres with a concentration of 1.08 x 10^9 parts per mL and a 2.08 x 10^{-5} M concentration of Trypan Blue. The red squares depict expected values computed from Mie theory. (g_{HG} = 0.933).

In summary, the automation provided by OPT 3.1 allows determination of desired optical properties in a matter of minutes within system hardware limits. Once the aforementioned outstanding issues have been resolved, the next phase of testing will be performed on actual biological tissue. Eventually the data collected using this system will be used to model light interaction with biological tissue.

Acknowledgments

This work was supported by the Engineering Science and Technology Division (ESTD) of the Oak Ridge National Laboratory and the Department of Energy, Office of Science. I would especially like to thank my mentor Justin Baba whose help and advice went well beyond the scope of the work presented here. I would also like to thank Philip Boudreaux for his help and the work he did to begin this project as well as Janakiramanan Ramachandran and Kelly Christian for their work on the refractive index portion of this project and everyone else in the ESTD for their help and making my time there very enjoyable.

References

[1] S. Prahl, "Optical Property Measurements Using the Inverse Adding-Doubling Program," [Online document], http://omlc.ogi.edu/pubs/pdf/man_iad.pdf, Accessed 03/19/08.

[2] SphereOptics, "Integrating Sphere Design and Applications," [Online Product Documentation], http://www.sphereoptics.com/assets/sphere-optic-pdf/sphere-technical-guide.pdf, Accessed 03/19/08.

[3] S. Prahl, Light Transport in Tissue, Dissertation, The University of Texas, Austin, 1988. Available: http://omlc.ogi.edu/pubs/pdf/prahl88.pdf, Accessed 03/19/08.

[4] Wikipedia, "Beer-Lambert law," Wikipedia. The Free Encyclopedia., [Online document], http://en.wikipedia.org/wiki/Beer-Lambert_law, Accessed 03/19/08.

[5] S. Prahl, "Mie Scattering," [Online resource], http://omlc.ogi.edu/calc/mie_calc.html, Accessed 03/19/08.

[6] F.A. Jenkins and H.E. White, Fundamentals of Optics, 4th ed., McGraw Hill, Inc., 1976.

[7] Dojindo, "Cellstain-Trypan Blue, Product code: T375-10," [Online documentation], http://www.dojindo.com/products/alphasearch/dojindodtl1.cfm?alphafield=Trypan%20Blue&ProdName=-Cellstain-%20Trypan%20Blue, Accessed 03/19/08.

[8] T. Vo-Dinh, Biomedical Photonics Handbook, Boca Raton, CRC Press, pp. 2.1–2.10, 2003.